Author(s): Marlo, M. & Alatalo, M. & Harju, A. & Nieminen, Risto M.

Title: Lateral diatomic two-dimensional artificial molecules: Classical transitions and quantum-mechanical counterparts

Year: 2002

Version: Final published version

Please cite the original version:

Marlo, M. & Alatalo, M. & Harju, A. & Nieminen, Risto M. 2002. Lateral diatomic two-dimensional artificial molecules: Classical transitions and quantum-mechanical counterparts. Physical Review B. Volume 66, Issue 15. 155322/1-7. ISSN 1550-235X (electronic). DOI: 10.1103/physrevb.66.155322.

Lateral diatomic two-dimensional artificial molecules: Classical transitions and quantum-mechanical counterparts

M. Marlo,* M. Alatalo, A. Harju, and R. M. Nieminen
Laboratory of Physics, Helsinki University of Technology, P. O. Box 1100, FIN-02015 HUT, Finland
(Received 21 December 2001; revised manuscript received 22 April 2002; published 23 October 2002)

Structural properties of a finite number ($N=2-20$) of point charges (classical electrons) confined laterally in a two-dimensional two-minima potential are calculated as a function of the distance (d) between the minima. The particles are confined by identical parabolic potentials and repel each other through a Coulomb potential. Both ground-state and metastable electron configurations are discussed. Discontinuous transitions from one configuration to another as a function of d are observed for $N=6$, 8, 11, 16, 17, 18, and 19. We show that the structural transitions have quantum-mechanical counterparts also in the limit of noninteracting electrons.

DOI: 10.1103/PhysRevB.66.155322 PACS number(s): 73.22.−f, 36.90.+f, 61.46.+w

I. INTRODUCTION

Quantum dots (sometimes called artificial atoms) are nanoscale semiconductor structures where a small number of electrons are confined into a small spatial region.[1,2] The electron motion is usually further restricted to two dimensions. There is strong theoretical evidence for the existence of a limit where the electron system crystallizes to Wigner molecules, which is seen as the localization of the electron density around positions that minimize the Coulomb repulsion.[3–9] In the limit of weak confinement (low density) or a very strong magnetic field the quantum effects are quenched or obscured and the electron correlations start to dominate the properties of the system. The ultimate limit is a purely classical system where only the Coulomb repulsion between the electrons defines the ground state. The problem reduces to finding the classical positions of electrons (which depend on the forms of the confining and the interaction potentials) that minimize the total energy of the system. One should also note as pointed out by Harju *et al.*,[7] based on accurate quantum-mechanical calculations, that a correlated many-electron system in a quantum dot can well be described in terms of independent electrons oscillating around their classical positions. This picture is energetically very accurate far beyond the confinement values where the system shows Wigner-molecule-like behavior.

There is growing interest in calculating[10–17] and measuring[18–20] the properties of coupled quantum dots. Due to the two-dimensional (2D) nature of quantum dots the two-atom system is different whether the quantum dots are coupled in the plane in which the electrons are confined (laterally coupled) or in the perpendicular direction (vertically coupled). Especially for laterally coupled quantum dots only a limited number of studies have appeared.[13–17]

Classical studies serve as a good starting point for more demanding quantum-mechanical calculations. Moreover, the study of classical electrons in vertically coupled artificial atoms has revealed interesting structural transitions in the ground-state electron configurations as a function of the distance between the atoms.[21]

Apart from quantum dots in the classical limit the point charges in two dimensions can be used to model also other physical systems. Examples include vortex lines in superconductors and superfluids and electrons on the surface of liquid He (see Ref. 22, and references therein). In the theoretical field, the ground state configurations of a confined classical 2D electron system have been studied in the case of a single artificial atom in Refs. 22–28 and for the vertically coupled artificial atom molecule as a function of the interatom distance in Ref. 21. Recently, also some experimental studies of 2D confined charged classical particle systems have appeared to reflect the classical cluster patterns in two dimensions.[29,30]

Classical point charges in a two-dimensional infinite plane crystallize into a hexagonal lattice at low temperatures. Parabolic confinement in the artificial atom, on the other hand, favors circularly symmetric solutions. The ground-state configuration is thus determined by two competing effects, circular symmetry and hexagonal coordination, resulting in nontrivial particle configurations. The reported configurations of the electron clusters in a single artificial atom do not all agree between different studies. The differences can be partly explained by the different forms of confinement and interaction potentials. However, when the number of particles, N, confined in the atom is one of the following, $N=2-5,7,10,12,14$, and 19, all results are in agreement while differences appear for $N=6,8,9,11,13,15-18$, and 20 (for $N\leqslant 20$).[22–30]

In this paper we consider two laterally coupled artificial atoms and we mainly focus on classical electrons in the artificial molecule. The changes in the ground-state electron configurations are studied for $N=2-20$ electrons in the molecule as the interatom distance is changed. The energies of the metastable states are also calculated at different distances and their role in the structural transitions in the ground-state electron configurations is discussed. We also show an interesting similarity between the classical structural transition and the quantum-mechanical one for the $N=6$ case.

II. MODEL AND METHODS

The commonly used quantum-mechanical Hamiltonian for N electrons in a two-dimensional structure can be written as

$$H=\sum_{i=1}^{N}\left(-\frac{\hbar^2}{2m^*}\nabla_i^2+V(\mathbf{r}_i)\right)+\frac{e^2}{4\pi\epsilon_0\epsilon}\sum_{i<j}\frac{1}{r_{ij}}, \quad (1)$$

where V is the external confining potential taken to be

$$V(\mathbf{r})=\frac{m^*\omega^2}{2}(\min[(x-d/2)^2,(x+d/2)^2]+y^2).$$

The electrons are described with coordinates $\mathbf{r}_i=(x_i,y_i)$ in two-dimensional space. The harmonic confinements are positioned symmetrically around the origin with distance d between the minima. m^* is the electron effective mass, ω the confinement strength, and ϵ the dielectric constant.

We mainly consider the classical limit ($\hbar\to 0$) of the model, where each electron reduces to a classical point charge. In the classical limit we study electron configurations as the distance between the minima is changed. In addition to the classical limit we also consider the quantum-mechanical limit of noninteracting electrons ($\epsilon\to\infty$). Our main interest is to show that similar structural transitions as seen in the classical limit can be found in the quantum case, even in the limit where interactions are not taken into account.

A. Monte Carlo simulation of classical limit

The minimum energy as a function of the positions of the particles, $E_{tot}=\min E(\mathbf{r}_1,\ldots,\mathbf{r}_N)$, is solved with a standard Metropolis Monte Carlo method[31] starting from a randomly chosen initial electron configuration $\mathbf{r}_1,\ldots,\mathbf{r}_N$. The accuracy and simulation time needed with the Metropolis algorithm was found to be quite sufficient for the current problem. We compared the calculated energies in the limit of a single artificial atom to those given in Ref. 22, and the results were found to be in complete agreement within the given accuracy.

In the simulations we choose four different distances between the minima and perform 300 test runs at each particle number ($N=2-20$) and distance ($d=0$, 200, 600, and 1000 Å). In addition to minimum-energy configurations we also obtain metastable states that are higher in energy compared to the ground state.

When the ground and metastable states are obtained at $d=0$, 200, 600, and 1000 Å we study the structural transitions between ground-state electron configurations at the intermediate distances. The electron configurations obtained from the fixed d calculations are taken as an input to Monte Carlo minimizations where the attempt step is set so small that the electron configuration cannot change to another. Then the distance is slightly altered ($d\to d\pm 1$ Å) and a new energy with slightly modified positions is calculated for the configuration defined by the input. The calculated new configuration is taken as an input to the next calculation with a new distance between the atoms, and so all distances between $d=0$, 200, and 600 Å are well sampled. However, it may happen that a configuration becomes unstable as the distance is changed. In that case the simulation converges to some other stable configuration, which can be seen as a sudden jump to a new energy value in the $E(d)$ plots. The energies of all states are studied as a function of the distance, and structural transitions in the ground-state configurations are examined.

In the classical calculations we measure the energy in meV and distance in Å. The confinement strength was set to $\hbar\omega=3$ meV and typical GaAs parameters were chosen to the effective mass and the dielectric constant: $m^*=0.067m_e$ and $\epsilon=13$. The calculated energy values and distances could be scaled to correspond to different values of ω, m^*, and ϵ, but changing the parameters also changes the effective distance between the minima, d, and then the minimum-energy configuration may not be the same anymore. Therefore we have have one significant parameter in the system, d, which scales as $\propto(m^*\omega^2\epsilon)^{-1/3}$.

III. RESULTS

A. Classical electron configurations

The results for the ground and metastable states are summarized in Table I. The ground-state energy per particle, E/N, and the corresponding configuration at three distances between the artificial atoms is represented in the row following the particle number N. If there exist metastable states at the given N and d, the energy difference $\Delta E/N$ to the ground-state and the electron configurations for the metastable state are also reported. However, not all metastable configurations are marked in Table I, since when starting the simulation from random positions more electrons can be trapped in one artificial atom than in the other. Only metastable states with either the same number of electrons per atom (for even N) or only one more at one than the other atom (for odd N) are reported. The notation for the configurations in a single artificial atom is chosen so that electrons are thought to be organized in (nearly) concentric shells around the potential minimum: (N_1,N_2,N_3), where N_1 denotes the number of electrons in the innermost shell, N_2 the next shell, and N_3 the number of electrons in the outermost shell. (For $N\leqslant 20$ only three shells are occupied). For the laterally coupled two-atom artificial molecule we have chosen the following notation for configurations: At $d=200$ Å the configuration is marked as if it would still be on a single atom centered around the midpoint connecting the two atoms. At $d=600$ Å the configurations are given as configurations of two separated atoms. The results for $d=1000$ Å are not presented in Table I, as they correspond to two isolated dots and the configurations can be deduced from the $d=0$ case. Also the excitation energies are very close to ones found in the case of a single dot. The only exceptions are the $N=15$, 16, and 17 cases that have excitation from the ground-state configuration (1,7) to a metastable one (2,6), not seen at $d=0$.

As Table I and Fig. 1(a) indicate, with eight particles in the single artificial atom ($d=0$ Å) the ground state is (1,7), one electron in the center and seven electrons in the circular shell, and there exist no metastable states. At $d=200$ Å a new ground state has appeared with a configuration (2,6) [Fig. 1(b)] while (1,7) has changed to a metastable state with excitation energy $+0.016$ meV (see Table I). At distances

TABLE I. Ground-state and metastable configurations and corresponding energies in meV/particle at three of the studied distances ($d=0$, 200, 600 Å). The energies of metastable states, $\Delta E/N$, are given as meV/particle above the ground-state energy. The configurations of electron clusters in the two-atom molecule are described with concentric shells located around the center of the system at $d=0$ and 200 Å and as two separate electron clusters located near the minimum of one of the two atoms at $d=600$ Å. See text for descriptions of configurations with asterisks.

	$d=0$ Å		$d=200$ Å		$d=600$ Å	
N	E/N (meV)	configuration	E/N (meV)	configuration	E/N (meV)	configuration
2	2.736	(2)	1.777	(2)	0.875	(1)(1)
3	4.780	(3)	3.894	(3)	2.940	(1)(2)
4	6.696	(4)	5.588	(4)	4.351	(2)(2)
5	8.531	(5)	7.340	(5)	5.915	(2)(3)
	+0.099	(1,4)				
6	10.231	(1,5)	8.939	(6)	7.234	(3)(3)
	+0.074	(6)	+0.033	(1,5)		
7	11.816	(1,6)	10.459	(1,6)	8.664	(3)(4)
8	13.384	(1,7)	11.933	(2,6)	9.932	(4)(4)
			+0.016	(1,7)	+0.003	(4)(4)
9	14.913	(2,7)	13.335	(2,7)	11.246	(4)(5)
	+0.022	(1,8)				
10	16.361	(2,8)	14.680	(2,8)	12.441	(5)(5)
	+0.012	(3,7)				
11	17.746	(3,8)	16.053	(3,8)	13.701	(5)(1,5)*
			+0.003	(2,9)		
12	19.111	(3,9)	17.354	(3,9)	14.873	(1,5)*(1,5)*
	+0.011	(4,8)	+0.004	(4,8)	+0.011	(1,5)*(1,5)
13	20.433	(4,9)	18.624	(4,9)	16.048	(1,5)*(1,6)
			+0.024	(4,9)		
14	21.738	(4,10)	19.854	(4,10)	17.168	(1,6)(1,6)
	+0.014	(5,9)				
15	23.010	(5,10)	21.072	(5,10)	18.302	(1,6)(1,7)
	+0.029	(1,5,9)	+0.035	(5,10)		
16	24.259	(1,5,10)	22.271	(6,10)	19.373	(1,7)(1,7)
	+0.009	(5,11)	+0.006	(5,11)		
17	25.473	(1,6,10)	23.448	(6,11)	20.468	(1,7)(2,7)
	+0.005	(1,5,11)	+0.010	(1,6,10)	+0.006	(1,7)(1,8)
			+0.016	(1,5,11)		
			+0.018	(6,11)		
18	26.660	(1,6,11)	24.597	(1,6,11)	21.522	(2,7)(2,7)
	+0.026	(1,7,10)	+0.006	(6,12)	+0.001	(1,8)(2,7)
19	27.841	(1,6,12)	25.728	(1,6,12)	22.572	(2,7)(2,8)
	+0.003	(1,7,11)	+0.004	(1,7,11)	+0.001	(1,8)(2,8)
			+0.016			
20	29.000	(1,7,12)	26.843		23.583	(2,8)(2,8)
	+0.024	(1,6,13)	+0.001			
			+0.003	(2,7,11)		

$d=600$ Å and $d=1000$ Å the notation is changed to two-atom configurations and for $N=8$ the ground state is marked with (4)(4), see Figs. 1(c) and 1(e).

The notation for configurations is not always exhaustive. The relative orientation of different shells and the relative orientations of the configurations of the two atoms are not always obvious. For example, when either or both atoms are left with four electrons ($N=7,8,9$), the orientation of the square(s) relative to the other atom changes as the distance is increased. At smaller distances the position of the square of four electrons is such that the tips of the squares are in the same line with the positions of the minima [see Fig. 1(c) for $N=8$ at $d=600$ Å]. As the distance is increased the square (or two squares with $N=8$) turns onto its side [see Fig. 1(e) for $N=8$ at $d=1000$ Å]. For $N=8$ at $d=600$ Å there also exists a metastable state where one of the squares is lying on

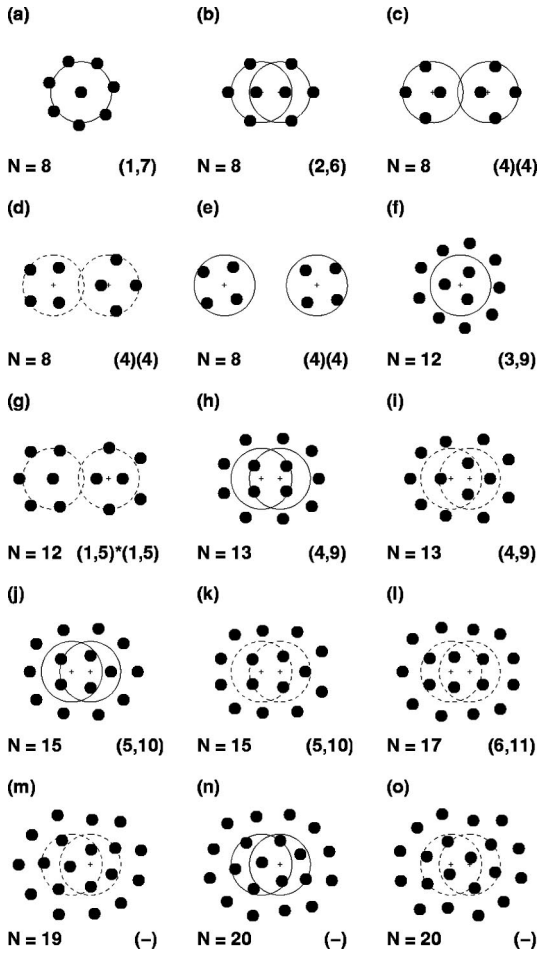

FIG. 1. Electron configurations of selected ground and metastable states. The configuration is marked on the lower right corner. To make it easier to distinguish different configurations and the distance between the minima ($d=0$, 200, 600, 1000 Å) a circle with 330-Å radius is plotted around each parabolic potential minimum. A dashed circle indicates a metastable state.

its side and the other on the tip [Fig. 1(d)]. Even though we divide electrons into shells in our notation it does not mean that the shells are strictly circular even for $d=0$. This can be seen clearly for $N=12$ in Fig. 1(f), where the outer shell looks more like an incomplete triangle with the tips missing. The configuration marked with $(1,5)^*$ in the two-atom configurations in Table I cannot be identified strictly to (6) but neither to (1,5). Therefore we choose the notation $(1,5)^*$ to describe the configuration. The difference between $(1,5)^*$ and (1,5) can be seen with the $(1,5)^*(1,5)$ metastable state in Fig. 1(g). The configurations of the ground and metastable states for $N=13$ at $d=200$ Å are marked in the same way in Table I, but are different as can be seen in Figs. 1(h) and 1(i). The same is true for $N=15$, Figs. 1(j) and 1(k). For the highest-energy metastable state for $N=17$, $d=200$ Å the two-atom notation would have described the configuration better, Fig. 1(l). One metastable state for $N=19$ and the ground state and one metastable state for $N=20$ at $d=200$ Å cannot be described with the shell structure notation. The configurations are depicted in Figs. 1(m)–1(o), respectively.

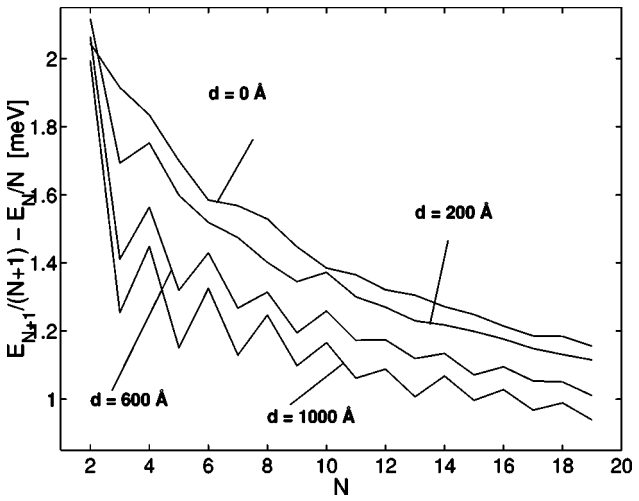

FIG. 2. Change in the chemical potential $[E_{N+1}/(N+1) - E_N/N]$ at $d=0$, 200, 600, and 1000 Å.

The changes in energy per particle of the ground states at the four studied distances as a function of N are shown in Fig. 2. At $d=0$ there are small troughs at $N=3$, 6, 10, and 17, at adding the fourth, seventh, eleventh and eighteenth particle. Moving to greater distances between the atoms, the change in the chemical potential is clearly peaked. Going to an odd number of particles increases the chemical potential much more than going to an even number of particles. Interesting is the intermediate distance of $d=200$ Å where this trend is observed for $N=2$–4 and 9–11, but otherwise the curve shows no clear structure and does not strictly follow the shape of the $d=0$-Å curve either.

B. Transitions

We now turn to study configurations between $d=0$, 200, and 600 Å. We start from all ground-state and metastable configurations and follow the energy of the configuration as a function of distance. As the distance between the atoms is increased it is not always clear whether the electrons just follow the two atoms drawn apart and continuously change to two separated atoms. Sometimes metastable states change to a ground state and the ground state to a metastable state as the distance between the atoms is increased. The clearest example can be seen in Table I for six electrons between $d=0$ and $d=200$ Å. At $d=0$ the (1,5) configuration is the ground state and (6) the metastable state. At $d=200$ Å it is the other way around: (6) is the ground and (1,5) a metastable state. The energy as a function of distance for two alternative configurations is shown in Fig. 3(a). The transition point, marked with a small circle, is at $d=111.6$ Å. The transition is continuous with respect to energy as a function of distance, but the curvature of the $E(d)$ curve is different and therefore the first derivative of energy with respect to d is discontinuous. Hereafter, by discontinuous structural transitions we mean the qualitative change in the ground-state electron configuration which is discontinuous with respect to $\partial E/\partial d$ at the transition point. For $N=8$, we find that at $d=135.9$ Å the electron configuration changes from (1,7) to

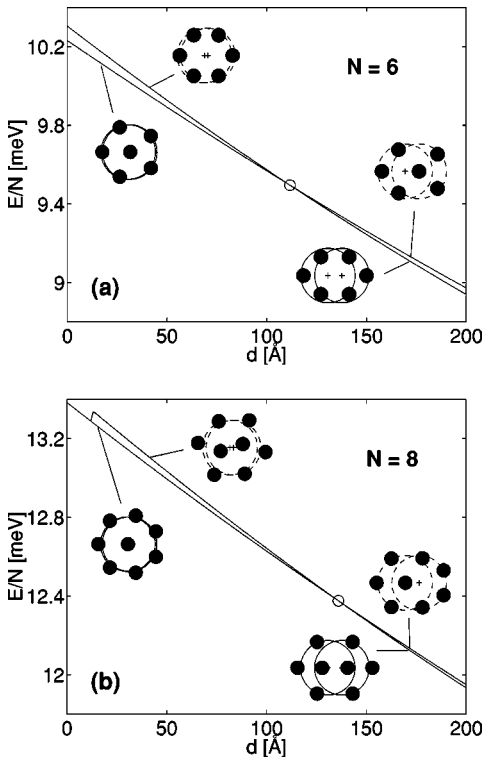

FIG. 3. Energy as a function of distance for $N=6$ and 8. The small circles indicate the discontinuous structural transition points.

(2,6), see Fig. 3(b). Notice that the (2,6) configuration is not stable at $d=0$ and becomes unstable below $d=17$ Å.

In addition to $N=6$ and 8, we find discontinuous transitions for $N=11$ and 16–19. All discontinuous transitions are summarized in Fig. 4 and Table II. These transitions can be divided into two main classes, namely, the ones at reasonably small interdot distances 100 Å$<d<$250 Å (type I, marked with ○) and the ones at large $d\approx$550 Å (type II, marked with ▷). The type-I transitions can be seen at $N=6$, 8, and 16–18. In all of these, the structure changes from a penta-, hexa- or heptagon structure with one electron inside the ring to a hexagonal ring, which can have either zero or two electrons inside the ring, the second case occurring only at $N=8$. The possibility of having just one electron inside the ring is not energetically favorable as the confinement potential has a maximum at the center.

The type-II transition occurring at $N=17$–19 can be characterized by a rotation of one of the two distant three-electron clusters in the inner shell of one of the atoms. Similar rotation but with four electrons can be seen in Figs. 1(c)–1(e) for $N=8$ and it is also seen for $N=7$ and 9. However, with small particle numbers, this rotation does not show any kinks in the ground-state energy curve and the rotation angle can also change continuously. For the triangles in the inner shells with $N=17$–19, on the other hand, we see only two alternative orientations: the tip is either pointing to the right or left and the transition between these two configurations is discontinuous. It is thus clear that the discontinuity in the rotations seen for $N=17$–19 results from the interaction of the rotating clusters with the surrounding electrons.

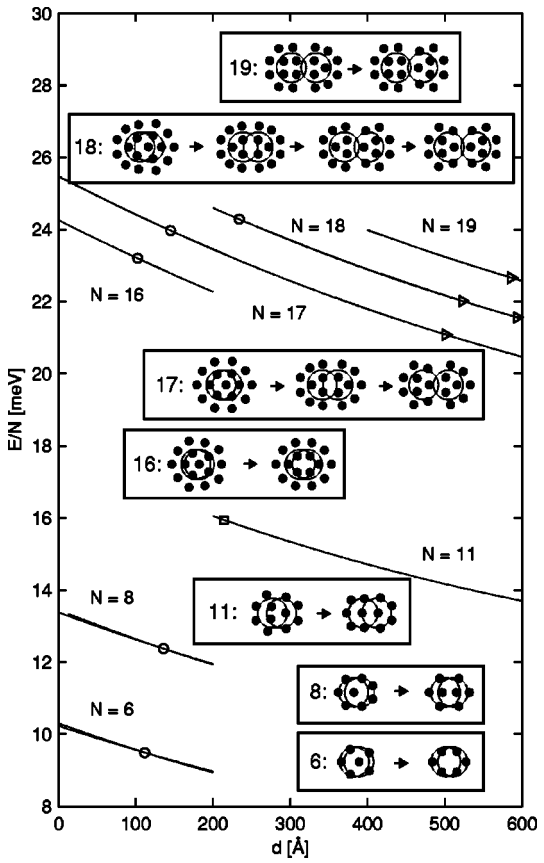

FIG. 4. E/N as a function of d for all N for which a discontinuous structural transition is observed. Transition points are denoted by symbols ○, ▷, and □ and changing ground-state configurations are depicted in boxes for each N. Energy differences between ground and metastable configurations are not distinguishable for $N>8$ in the figure.

For $N=11$ we observe quite surprisingly a discontinuous transition, which does not fall into either of the two classes of discontinuous transitions. It is even more interesting if we compare it to the continuous transition of $N=12$ in Fig. 5(a). The left-hand-side atom for $N=11$ in Fig. 4 and the left atom of the lower left configuration in Fig. 5(a) look similar, where of course the right atom has one more electron with $N=12$. However, for $N=12$ we have a continuous transition

TABLE II. Discontinuous structural transitions: ○, ▷, and □ specify the type of transition and d the transition point.

$N=19$	▷	(2,8)(1,8)	→	(2,8)(2,7)	$d=586.0$ Å
$N=18$	○	(1,6,11)	→	(6,12)	$d=233.9$ Å
	▷	(1,8)(1,8)	→	(1,8)(2,7)	$d=522.8$ Å
	▷	(1,8)(2,7)	→	(2,7)(2,7)	$d=593.4$ Å
$N=17$	○	(1,6,10)	→	(6,11)	$d=145.0$ Å
	▷	(1,7)(1,8)	→	(2,7)(1,7)	$d=501.1$ Å
$N=16$	○	(1,5,10)	→	(6,10)	$d=102.4$ Å
$N=11$	□	(3,8)	→	(2,9)	$d=214.2$ Å
$N=8$	○	(1,7)	→	(2,6)	$d=135.9$ Å
$N=6$	○	(1,5)	→	(6)	$d=111.6$ Å

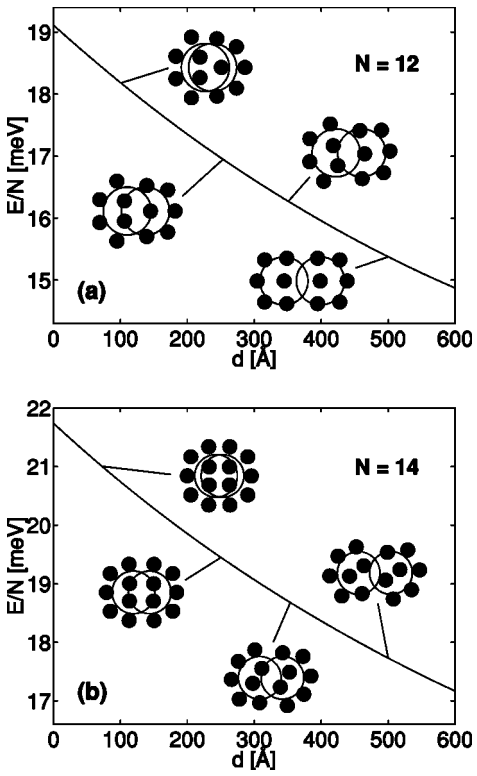

FIG. 5. Ground-state electron configurations along $E(d)$ curve for $N=12$ and 14.

whereas the transition for $N=11$ is discontinuous. The continuous rotation of the left atom with $N=11$ is not favorable whereas with $N=12$ it is the transition mechanism. The same continuous rotation as with $N=12$ is seen for $N=13$ with the six-electron atom and the seven-electron atom changing in a similar manner as both atoms in Fig. 5(b) with $N=14$. The rotation of the seven-electron atom with $N=15$ follows the similar transition as with $N=14$. For $N=20$ and 19 we do not observe type-I discontinuous transition at small interatom distances but increasing the distance transforms the configurations continuously in rather unsymmetric forms shown in Figs. 1(m) and 1(o).

C. Quantum-mechanical version of type-I transition

To show that the classical transitions are relevant even for the quantum case, we have studied the noninteracting quantum-mechanical $N=6$ case. The reason for this N is that it is the smallest particle number with a discontinuous transition of type I.

The noninteracting quantum-mechanical problem can be reduced to a one-dimensional one as the potential is separable, and the single-particle states of the transverse motion (y direction) are those of the simple harmonic oscillator with energy $\varepsilon_{n_y}=\frac{1}{2}+n_y$, where $n_y=0,1,2,\ldots$. The one-dimensional longitudinal part can easily be solved numerically. Combining the energies of the longitudinal part with the transverse ones, one obtains the spectra of Fig. 6. One can see that the energies are equal to those of the simple

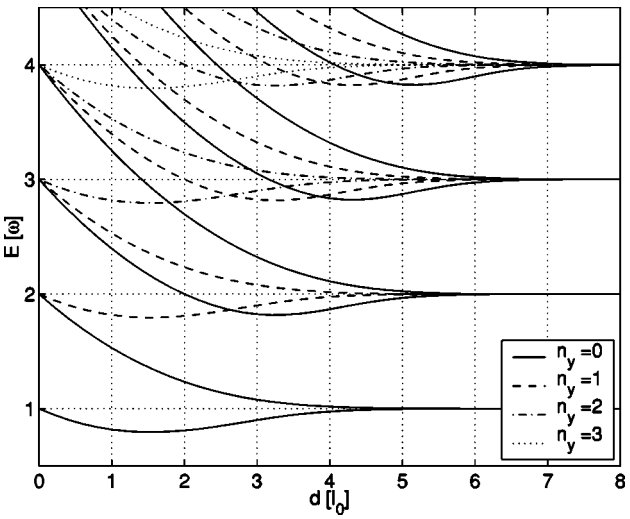

FIG. 6. Lowest single-particle energies as a function of the interdot distance d. The inset shows the quantum number of the transverse motion.

harmonic oscillator for $d=0$, and of two independent oscillators at large d. In the quantum-mechanical limit we measure the length in units of $l_0=\sqrt{\hbar/m^*\omega}$ and energy in units of $\hbar\omega$.

We drop the spin of the quantum-mechanical electrons, as it is not relevant in the classical limit. This corresponds to taking the system to be spin polarized. One can see from the energy levels shown in Fig. 6 that there exists one transition for this particle number. In this transition point, one electron moves from a bonding $n_y=2$ state to an antibonding $n_y=0$ state. In the classical limit, the electrons avoid each other due to the Coulomb interaction. In our noninteracting quantum-mechanical case, the electron-electron repulsion results from the Pauli principle.

When the quantum-mechanical system approaches the classical limit, the most probable configuration $\mathbf{R}^*$, maximizing the density $|\Psi(\mathbf{R})|^2$, approaches the classical elec-

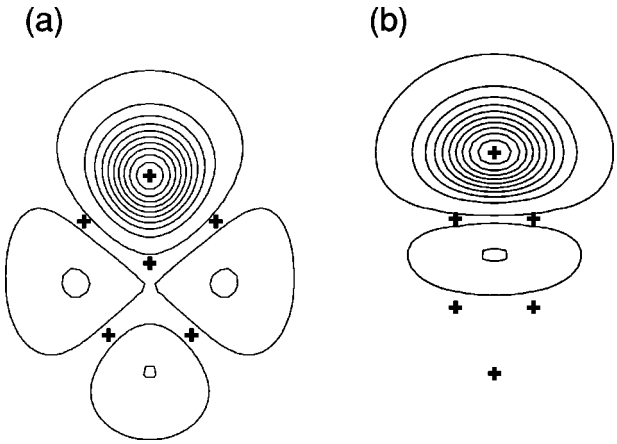

FIG. 7. Conditional probability densities and the most probable electron positions (marked with plus signs). The left (right) panel corresponds to a small (large) interdot distance d, correspondingly. The contours are uniformly from 0.01 to 0.91.

tron positions. The quantum effects and the transition to the classical limit are most conveniently studied using the single-particle probability distribution $\tilde{\rho}(\mathbf{r})$,[7] defined as

$$\tilde{\rho}(\mathbf{r}) = \left| \frac{\Psi(\mathbf{r}, \mathbf{r}_2^*, \ldots, \mathbf{r}_N^*)}{\Psi(\mathbf{r}_1^*, \mathbf{r}_2^*, \ldots, \mathbf{r}_N^*)} \right|^2, \tag{2}$$

where the coordinates $\mathbf{r}_i^*$ are fixed to the ones from the most probable configuration $\mathbf{R}^*$. In approaching the classical limit, the density $\tilde{\rho}(\mathbf{r})$ is more and more peaked around the classical position $\mathbf{r}_1^*$, still showing quantum fluctuations, as seen in the case of a single quantum dot.[7]

We now take the quantum model to the opposite limit of the classical one where the information of the classical positions might be stored in the coordinates of the most probable electron configuration. One can see in Fig. 7, which shows the $\tilde{\rho}(\mathbf{r})$ for the two ground states that this is really the case. It is very interesting to see that the most probable electron positions change in the transition point very similarly to the classical case. We see clearly a transition of type I. It is highly nontrivial that the electron triangles for the large-d case are facing the same way as in the classical case. Our quantum-mechanical analysis of the $N=6$ case shows that at least the type-I transitions are very relevant for quantum dot molecules also beyond the classical limit.

IV. SUMMARY

To summarize, we have calculated ground- and metastable state configurations of classical point charges confined in two dimensions within two laterally coupled parabolic potentials. The ground and metastable electron configurations are studied as a function of the distance between the atoms. Discontinuous (in $\partial E/\partial d$) transitions in the ground-state configurations were observed for $N=6,8,11$, and 16–19. We have analyzed these transitions in detail, and grouped them according to two main categories. We have found a quantum-mechanical counterpart for one type of transition. The configurations of purely classical electrons in laterally coupled two-minima potential have an interesting and complex spectrum as the distance between the minima is changed.

ACKNOWLEDGMENTS

This work has been supported by the Academy of Finland through its Centers of Excellence Program (2000-2005).

*Electronic address: Meri.Marlo@hut.fi

[1] R. Ashoori, Nature (London) **379**, 413 (1996).
[2] M.A. Kastner, Phys. Today **46**, 24 (1993).
[3] R. Egger, W. Häusler, C.H. Mak, and H. Grabert, Phys. Rev. Lett. **82**, 3320 (1999).
[4] S.M. Reimann, M. Koskinen, and M. Manninen, Phys. Rev. B **62**, 8108 (2000).
[5] C.E. Creffield, W. Häusler, J.H. Jefferson, and S. Sakar, Phys. Rev. B **59**, 10 719 (1999).
[6] B. Reusch, W. Häusler, and H. Grabert, Phys. Rev. B **63**, 113313 (2001).
[7] A. Harju, S. Siljamäki, and R.M. Nieminen, Phys. Rev. B **65**, 075309 (2002).
[8] M. Koskinen, M. Manninen, and S.M. Reimann, Phys. Rev. Lett. **79**, 1389 (1997).
[9] P.A. Maksym, H. Imamura, G.P. Mallon, and H. Aoki, J. Phys.: Condens. Matter **12**, R299 (2000).
[10] H. Imamura, P.A. Maksym, and H. Aoki, Phys. Rev. B **59**, 5817 (1999).
[11] S. Nagaraja, J.-P. Leburton, and R.M. Martin, Phys. Rev. B **60**, 8759 (1999).
[12] B. Partoens and F.M. Peeters, Phys. Rev. Lett. **84**, 4433 (2000).
[13] A. Harju, S. Siljamäki, and R.M. Nieminen, Phys. Rev. Lett. **88**, 226804 (2002).
[14] T. Chakraborty, V. Halonen, and P. Pietiläinen, Phys. Rev. B **43**, 14 289 (1991).
[15] A. Wensauer, O. Steffens, M. Suhrke, and U. Rössler, Phys. Rev. B **62**, 2605 (2000).
[16] J. Kolehmainen, S.M. Reimann, M. Koskinen, and M. Manninen, Eur. Phys. J. B **13**, 731 (2000).
[17] C. Yannouleas and U. Landman, Eur. Phys. J. D **16**, 373 (2001).
[18] C. Livermore, C.H. Crouch, R.M. Westervelt, K.L. Campman, and A.C. Gossard, Science **274**, 1332 (1996).
[19] T.H. Oosterkamp, T. Fujisawa, W.G. van der Wiel, K. Ishibashi, R.V. Hijman, S. Tarucha, and L.P. Kouwenhoven, Nature (London) **395**, 873 (1998).
[20] M. Brodsky, N.B. Zhitenev, R.C. Ashoori, L.N. Pfeiffer, and K.W. West, Phys. Rev. Lett. **85**, 2356 (2000).
[21] B. Partoens, V. Schweigert, and F. Peeters, Phys. Rev. Lett. **79**, 3990 (1997).
[22] M. Kong, B. Partoens, and F.M. Peeters, Phys. Rev. E **65**, 046602 (2002).
[23] F. Bolton and U. Rössler, Superlattices Microstruct. **13**, 139 (1993).
[24] V.M. Bedanov and F.M. Peeters, Phys. Rev. B **49**, 2667 (1994).
[25] Y.-J. Lai and L. I, Phys. Rev. E **60**, 4743 (1999).
[26] G. Date, M.V.N. Murthy, and R. Vathsan, J. Phys.: Condens. Matter **10**, 5875 (1998).
[27] L.J. Campbell and R.M. Ziff, Phys. Rev. B **20**, 1886 (1979).
[28] V.A. Schweigert and F.M. Peeters, Phys. Rev. B **51**, 7700 (1995).
[29] W.-T. Juan, Z.-H. Huang, J.-W. Hsu, Y.-J. Lai, and L. I, Phys. Rev. E **58**, R6947 (1998).
[30] M. Saint Jean, C. Even, and C. Guthmann, Europhys. Lett. **55**, 45 (2001).
[31] N. Metropolis, A.W. Rosenbluth, and A.H. Teller, J. Chem. Phys. **21**, 1087 (1953).